

Detecting Spectrum Opportunities in Poisson Primary Networks

Wei Ren and Qing Zhao

I. INTRODUCTION

Opportunistic spectrum access (OSA), also referred to as spectrum overlay, is one of the several approaches envisioned for dynamic spectrum management [1]. The basic idea of OSA is to allow secondary users to exploit temporarily and locally unused channels without causing unacceptable interference to primary users.

One of the central issues in OSA is spectrum opportunity detection through sensing. Before transmitting over a particular channel, a secondary user needs to decide whether this channel is an opportunity. This is the so-called “Listen-before-Talk” (LBT). In this report, to quantitatively characterize the performance of LBT, we consider a slotted network setup where primary users are distributed according to a spatial Poisson process (see Sec. II). We first analyze the performance of LBT at both physical and MAC layers, and then we investigate the translation from physical layer opportunity detection performance to MAC layer performance, which is crucial in the design of the opportunity detector. In particular, we demonstrate the complex dependency of the relationship between PHY and MAC on the application type (guaranteed delivery vs. best-effort delivery) and the use of handshaking signaling such as RTS/CTS at the MAC layer.

Throughout the report, we use capital letters for parameters of primary users and lower-cased letters for secondary users.

II. NETWORK MODEL

Consider a decentralized primary network with slotted transmission structure. Assume that users are distributed according to a two-dimensional homogeneous Poisson process with density λ . At the beginning of each slot, each primary user has a probability p to transmit data to a

⁰This work was supported by the Army Research Laboratory CTA on Communication and Networks under Grant DAAD19-01-2-0011 and by the National Science Foundation under Grants CNS-0627090 and ECS-0622200.

receiver that is uniformly distributed within its transmission range R_p (see Fig. 1). Based on the Thinning Theorem and the Displacement Theorem for marked Poisson processes [2], both primary transmitters and receivers form a two-dimensional homogeneous Poisson process with density $p\lambda$. Note that these two Poisson processes are not independent.

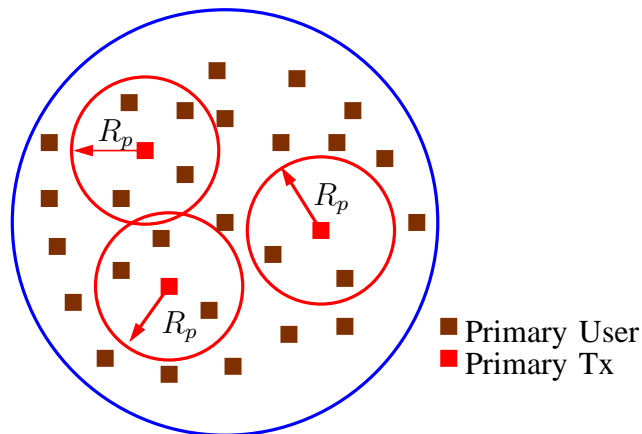


Fig. 1. A Poisson distributed primary network.

III. SPECTRUM OPPORTUNITIES: DEFINITION AND IMPLICATIONS

A rigorous study of spectrum opportunity detection must start from a clear definition of spectrum opportunity. In fact, the concept of spectrum opportunity is more involved than it at first may appear [3]. As illustrated in Fig. 2, a channel is an opportunity to a pair of secondary users A and B if they can communicate successfully while limiting the interference to primary receivers. More specifically, B can not be affected by primary transmitters, and A can not interfere with any primary receivers. In other words, there is no primary receiver located within distance r_I to A , and no primary transmitter within distance R_I to B , where r_I is the interference range of secondary users and is monotonically increasing in the transmission power p_{tx} , R_I is the interference range of primary users. Here we have adopted the disk model for signal propagation and interference. This definition, however, applies to general cases [5].

The first implication of the spectrum opportunity is that to detect the opportunity, A needs to detect the presence of nearby primary receivers, and B needs to detect the presence of nearby primary transmitters. However, without assuming cooperation from primary users, primary receivers are much more difficult to detect than primary transmitters. One effective alternative

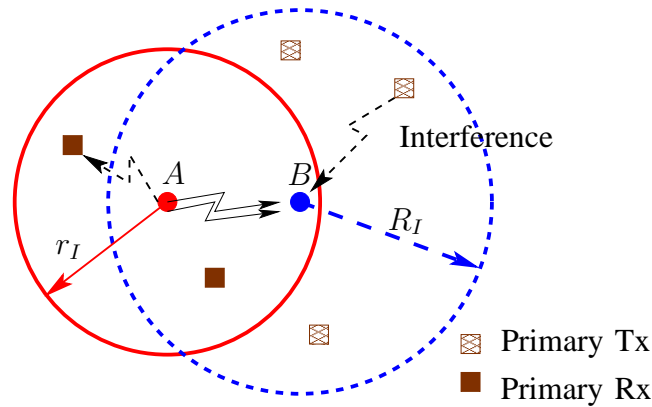


Fig. 2. Definition of spectrum opportunity.

is "listen-before-talk" which transforms the problem of detecting primary receivers to detecting primary transmitters. As shown in Fig. 3, A infers the presence of primary receivers within distance r_I from the presence of primary transmitters within distance r_D , where r_D denotes the detection range and can be adjusted by changing, for example, the threshold of an energy detector. Let R_p denote the transmission range of primary users, then the most conservative detection range is $R_p + r_I$, which may result in overlooked opportunities. As illustrated in Fig 3, if the detection range is $R_p + r_I$, the transmission activities of primary transmitter X will prevent A from accessing the spectrum opportunity even though the intended receiver of X is outside the interference range r_I of A . However, if we let $r_D < R_p + r_I$, e.g., the dashed circle in Fig. 2, A can not detect the transmission activity of Y , and it will interfere with the intended receiver of Y . So even if A uses LBT with "perfect ears", spectrum opportunity detection can not achieve perfect performance due to the fundamental deficiency of LBT.

The second implication is that spectrum opportunity is asymmetric, that is, a channel that is an opportunity when A is the transmitter and B the receiver may not be an opportunity when B is the transmitter and A the receiver. So if B needs to send back the acknowledgement to A after B receives data, the acknowledgement from B may not be received by A . This asymmetry leads to a complex relationship between the opportunity detection performance at the physical layer and the link throughput and interference constraint at the MAC layer. As shown in Sec. ?? and Sec. V-D, this relationship varies with the application type (for example, whether acknowledgement is needed to complete a successful data transmission) and the use of

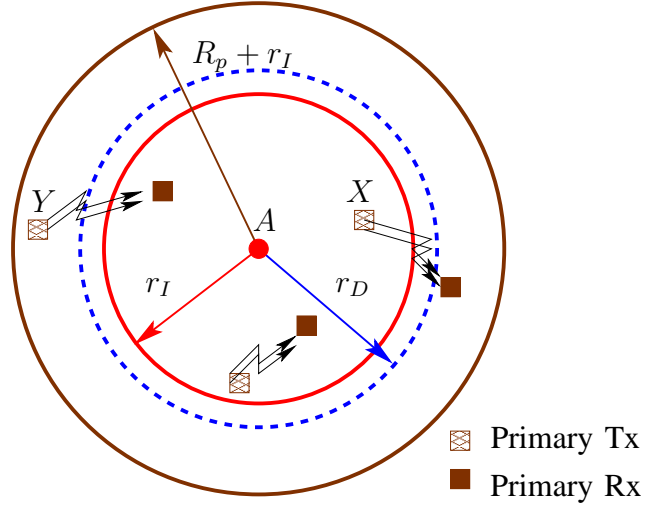


Fig. 3. Spectrum opportunity detection at the secondary tx

handshaking signaling. In other words, it depends on whether the roles of the transmitter and receiver need to be reversed during the process of communicating a data packet.

IV. SPECTRUM OPPORTUNITY DETECTION: FIGURES OF MERIT

In this section, we specify the figures of merit for spectrum opportunity detection.

PHY Performance. The spectrum opportunity detection can be formulated as a binary hypothesis testing problem. Let $\mathbb{I}(A, d, \text{rx})$ denote the presence of primary receivers within distance d to the secondary transmitter A , and $\mathbb{I}(B, d, \text{tx})$ the presence of primary transmitters within distance d to the secondary receiver B . Let $\overline{\mathbb{I}(\cdot, \cdot, \cdot)}$ denote the complement of $\mathbb{I}(\cdot, \cdot, \cdot)$. The two hypotheses are given by

\mathcal{H}_0 : opportunity exists, *i.e.*, $\overline{\mathbb{I}(A, r_I, \text{rx})} \cap \overline{\mathbb{I}(B, R_I, \text{tx})}$.

\mathcal{H}_1 : no opportunity, *i.e.*, $\mathbb{I}(A, r_I, \text{rx}) \cup \mathbb{I}(B, R_I, \text{tx})$.

The figures of merit at the physical layer are given by the probabilities of false alarm P_F and miss detection P_{MD} :

$$P_F \triangleq Pr\{\text{decide } \mathcal{H}_1 \mid \mathcal{H}_0\}, \quad P_{MD} \triangleq Pr\{\text{decide } \mathcal{H}_0 \mid \mathcal{H}_1\}.$$

The performance of the detector is specified by the receiver operating characteristic (ROC) curve, which gives $1 - P_{MD}$ (probability of detection or detection power denoted by P_D) as a function

of P_F . See Fig. 4 for an illustration. In general, reducing P_F comes at a price of increasing P_{MD} and *vice versa*. The tradeoff between false alarm and miss detection is thus crucial, and the operating characteristics of the spectrum sensor should be designed by considering the impact of detection errors on the MAC performance. As a consequence, the relationship between PHY and MAC needs to be carefully examined. In particular, as for LBT with perfect ears (see Fig. 3), the tradeoff between false alarm and miss detection can be achieved by adjusting the detection range $r_D \in (0, r_I + R_p]$.

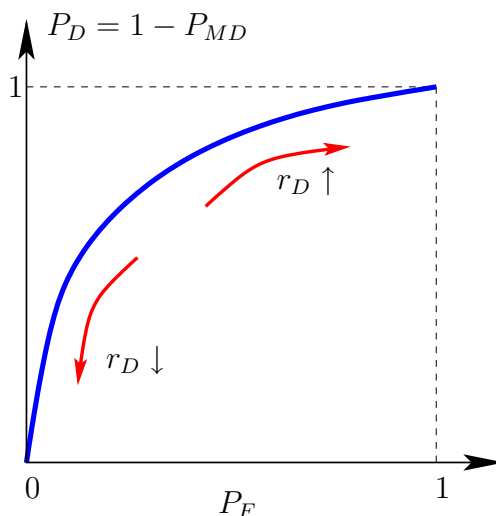


Fig. 4. ROC curve of LBT with perfect ears.

MAC Performance The MAC layer performance is measured by the throughput of the secondary user and the interference to the primary users. The design objective is to maximize the throughput of secondary users while limiting the interference to the primary users.

The figures of merit at the MAC layer are thus given by the probability P_S of successful data transmission and the probability P_C of colliding with primary users¹.

$$P_S = Pr\{\text{successful data transmission}\}, \quad (1)$$

$$P_C = Pr\{A \text{ transmits data} \mid \mathbb{I}(A, r_I, \text{rx})\}. \quad (2)$$

¹We assume that collisions with primary users are caused by data transmissions. We ignore the interference from the transmission of acknowledgement and handshaking signaling such as RTS/CTS due to their short duration.

Note that P_C is conditioned on $\mathbb{I}(A, r_I, \mathbf{rx})$ instead of \mathcal{H}_1 . Clearly, $\Pr[\mathbb{I}(A, r_I, \mathbf{rx})] \leq \Pr[\mathcal{H}_1]$. This further complicates the relationship between P_{MD} and P_C as shown in Sec. V.

V. PERFORMANCE OF LBT WITH PERFECT EARS

In this section, we analyze the performance of LBT with perfect ears in a Poisson distributed primary network. First, since false alarm and miss detection are conditioned on \mathcal{H}_0 and \mathcal{H}_1 respectively, we derive the expression for the probability of spectrum opportunity $Pr[\mathcal{H}_0]$. Second, based on the expression for $Pr[\mathcal{H}_0]$, we obtain the analytical expressions for PHY performance measures (false alarm probability P_F , miss detection probability P_{MD}) and MAC performance measures (successful transmission probability P_S , collision probability P_C). Last, we compare applications requiring guaranteed delivery with those relying on best effort (for example, media streaming and network gaming), and also study the impact of MAC handshaking signaling on the performance of LBT.

A. Probability of Spectrum Opportunity $Pr[\mathcal{H}_0]$

Recall the definition of the conditional probability,

$$\begin{aligned} Pr[\mathcal{H}_0] &= Pr\{\overline{\mathbb{I}(A, r_I, \mathbf{rx})} \cap \overline{\mathbb{I}(B, R_I, \mathbf{tx})}\}, \\ &= Pr\{\overline{\mathbb{I}(A, r_I, \mathbf{rx})} \mid \overline{\mathbb{I}(B, R_I, \mathbf{tx})}\} \cdot Pr\{\overline{\mathbb{I}(B, R_I, \mathbf{tx})}\}. \end{aligned} \quad (3)$$

Next we will calculate the two probabilities in the above expression one by one.

$$\square Pr\{\overline{\mathbb{I}(B, R_I, \mathbf{tx})}\}$$

Since primary transmitters satisfy a Poisson process with density $p\lambda$, it is easy to see that

$$Pr\{\overline{\mathbb{I}(B, R_I, \mathbf{tx})}\} = \exp(-p\lambda_B), \quad (4)$$

where $\lambda_B = \lambda\pi R_I^2$.

$$\square Pr\{\overline{\mathbb{I}(A, r_I, \mathbf{rx})} \mid \overline{\mathbb{I}(B, R_I, \mathbf{tx})}\}$$

Let d be the distance between A and B , $\mathcal{S}_c(d, r_1, r_2)$ denote the area within a circle with radius r_1 centered at A but outside the circle with radius r_2 centered at B . The area of $\mathcal{S}_c(d, r_1, r_2)$ equals $\pi r_1^2 - \mathcal{S}_I(d, r_1, r_2)$, where $\mathcal{S}_I(d, r_1, r_2)$ is the common area of two circles with radius r_1

and r_2 and centered d apart (see Appendix A for its expression). Then by considering the fact that the primary receiver within r_I of A can only communicate with the primary transmitter within $r_I + R_p$ of A and using the Total Probability Theorem, we have that

$$\begin{aligned}
 & Pr\{\overline{\mathbb{I}(A, r_I, \mathbf{rx})} \mid \overline{\mathbb{I}(B, R_I, \mathbf{tx})}\} \\
 &= \sum_{k=0}^{\infty} Pr\{\overline{\mathbb{I}(A, r_I, \mathbf{rx})} \cap (k \text{ tx} \in \mathcal{S}_c(d, r_I + R_p, R_I)) \mid \overline{\mathbb{I}(B, R_I, \mathbf{tx})}\}, \\
 &= \sum_{k=0}^{\infty} Pr\{\overline{\mathbb{I}(A, r_I, \mathbf{rx})} \mid (k \text{ tx} \in \mathcal{S}_c(d, r_I + R_p, R_I)) \cap \overline{\mathbb{I}(B, R_I, \mathbf{tx})}\} \\
 &\quad \cdot Pr\{k \text{ tx} \in \mathcal{S}_c(d, r_I + R_p, R_I)\}.
 \end{aligned} \tag{5}$$

Here " $k \text{ tx} \in \mathcal{S}_c(d, r_I + R_p, R_I)$ " means that there exist k primary transmitters inside the region $\mathcal{S}_c(d, r_I + R_p, R_I)$. In the last step, we use the fact that the spatial distribution of primary transmitters in $\mathcal{S}_c(d, r_I + R_p, R_I)$ is independent with that in the R_I circle of B .

Similarly to $Pr\{\overline{\mathbb{I}(B, R_I, \mathbf{tx})}\}$, $Pr\{k \text{ tx} \in \mathcal{S}_c(d, r_I + R_p, R_I)\}$ is given by

$$Pr\{k \text{ tx} \in \mathcal{S}_c(d, r_I + R_p, R_I)\} = \frac{(p\lambda_{A1})^k}{k!} \exp(-p\lambda_{A1}), \tag{6}$$

where $\lambda_{A1} = \lambda_{\mathcal{S}_c(d, r_I + R_p, R_I)}$.

Let $P_1 = Pr\{\mathbb{I}(A, r_I, \mathbf{rx}) \mid (\text{one tx} \in \mathcal{S}_c(d, r_I + R_p, R_I)) \cap \mathbb{I}(B, R_I, \mathbf{tx})\}$, then since each primary transmitter choose its receiver independently, it follows that

$$\begin{aligned}
 & Pr\{\mathbb{I}(A, r_I, \mathbf{rx}) \mid (k \text{ tx} \in \mathcal{S}_c(d, r_I + R_p, R_I)) \cap \mathbb{I}(B, R_I, \mathbf{tx})\} \\
 &= P_1^k = \left(\iint_{\mathcal{S}_c(d, r_I + R_p, R_I)} \frac{1}{\mathcal{S}_c(d, r_I + R_p, R_I)} \left[1 - \frac{\mathcal{S}_I(r, R_p, r_I)}{\pi R_p^2} \right] r dr d\theta \right)^k.
 \end{aligned} \tag{7}$$

Here r is the radial coordinate in the polar coordinate system, and θ is the angular coordinate.

We choose the secondary transmitter A as the origin.

□ $Pr[\mathcal{H}_0]$

By combining (7), (6), (5), and (4) with (3), we can express the probability $Pr[\mathcal{H}_0]$ of hypothesis \mathcal{H}_0 in the following form.

$$\begin{aligned}
 Pr[\mathcal{H}_0] &= \exp[-p(\lambda_{A1}(1 - P_1) + \lambda_B)], \\
 &= \exp \left[-p\lambda \left(\iint_{\mathcal{S}_c(d, r_I + R_p, R_I)} \frac{\mathcal{S}_I(r, R_p, r_I)}{\pi R_p^2} r dr d\theta + \pi R_I^2 \right) \right].
 \end{aligned} \tag{8}$$

The detailed description of $\mathcal{S}_c(d, r_I + R_p, R_I)$ in the polar coordinate system is given in Appendix B. Note that the integrand $\frac{S_I(r, R_p, r_I)}{\pi R_p^2}$ does not depend on the angular coordinate θ , so by integrating with respect to θ first, we can reduce the double integral in (8) to a single integral $\int_0^{r_I + R_p} \frac{S_I(r, R_p, r_I)}{\pi R_p^2} r \cdot \theta(r) dr$, where $\theta(r)$ is a function of r and determined by the shape of $\mathcal{S}_c(d, r_I + R_p, R_I)$. If we take into account the symmetry of $\mathcal{S}_c(d, r_I + R_p, R_I)$, the computation can be further simplified.

B. PHY Performance

1) False Alarm Probability P_F :

For LBT, false alarm occurs if and only if the secondary transmitter A detects the presence of primary transmitters under \mathcal{H}_0 (see Fig. 5). In this case, false alarm probability P_F is given by

$$\begin{aligned} P_F &= Pr\{\mathbb{I}(A, r_D, \text{tx}) \mid \mathcal{H}_0\}, \\ &= 1 - Pr\{\overline{\mathbb{I}(A, r_D, \text{tx})} \mid \mathcal{H}_0\}. \end{aligned} \quad (9)$$

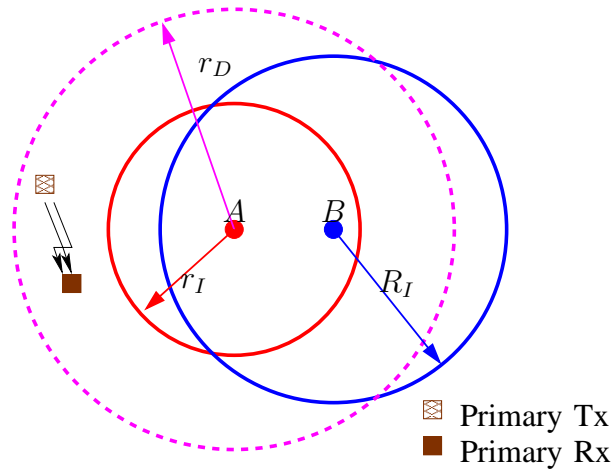


Fig. 5. An illustration of false alarm (Under \mathcal{H}_0 , there exist primary txs within r_D of A)

Use the Bayer Rule,

$$\begin{aligned} &Pr\{\overline{\mathbb{I}(A, r_D, \text{tx})} \mid \mathcal{H}_0\} \\ &= Pr\{\overline{\mathbb{I}(A, r_D, \text{tx})} \mid \overline{\mathbb{I}(A, r_I, \text{rx})} \cap \overline{\mathbb{I}(B, R_I, \text{tx})}\}, \\ &= \frac{Pr\{\overline{\mathbb{I}(A, r_I, \text{rx})} \mid \overline{\mathbb{I}(A, r_D, \text{tx})} \cap \overline{\mathbb{I}(B, R_I, \text{tx})}\} \cdot Pr\{\overline{\mathbb{I}(A, r_D, \text{tx})} \cap \overline{\mathbb{I}(B, R_I, \text{tx})}\}}{Pr[\mathcal{H}_0]}. \end{aligned} \quad (10)$$

Next we will calculate the two probabilities in the numerator of the above expression one by one.

$$\square Pr\{\overline{\mathbb{I}(A, r_D, \mathbf{tx})} \cap \overline{\mathbb{I}(B, R_I, \mathbf{tx})}\}$$

Similarly to $Pr\{\overline{\mathbb{I}(B, R_I, \mathbf{tx})}\}$, $Pr\{\overline{\mathbb{I}(A, r_D, \mathbf{tx})} \cap \overline{\mathbb{I}(B, R_I, \mathbf{tx})}\}$ is given by

$$Pr\{\overline{\mathbb{I}(A, r_D, \mathbf{tx})} \cap \overline{\mathbb{I}(B, R_I, \mathbf{tx})}\} = \exp(-p\lambda_{AB}), \quad (11)$$

where $\lambda_{AB} = \lambda[\pi(r_D^2 + R_I^2) - \mathcal{S}_I(d, r_D, R_I)]$.

$$\square Pr\{\overline{\mathbb{I}(A, r_I, \mathbf{rx})} \mid \overline{\mathbb{I}(A, r_D, \mathbf{tx})} \cap \overline{\mathbb{I}(B, R_I, \mathbf{tx})}\}$$

Use the Total Probability Theorem again,

$$\begin{aligned} & Pr\{\overline{\mathbb{I}(A, r_I, \mathbf{rx})} \mid \overline{\mathbb{I}(A, r_D, \mathbf{tx})} \cap \overline{\mathbb{I}(B, R_I, \mathbf{tx})}\} \\ &= \sum_{k=0}^{\infty} Pr\{\overline{\mathbb{I}(A, r_I, \mathbf{rx})} \cap [k \text{ tx} \in \mathcal{S}_c(d, r_I + R_p, R_I) - \mathcal{S}_{A2}] \mid \overline{\mathbb{I}(A, r_D, \mathbf{tx})} \cap \overline{\mathbb{I}(B, R_I, \mathbf{tx})}\}, \\ &= \sum_{k=0}^{\infty} Pr\{\overline{\mathbb{I}(A, r_I, \mathbf{rx})} \mid [k \text{ tx} \in \mathcal{S}_c(d, r_I + R_p, R_I) - \mathcal{S}_{A2}] \cap \overline{\mathbb{I}(A, r_D, \mathbf{tx})} \cap \overline{\mathbb{I}(B, R_I, \mathbf{tx})}\} \\ & \quad \cdot Pr\{k \text{ tx} \in \mathcal{S}_c(d, r_I + R_p, R_I) - \mathcal{S}_{A2}\}, \end{aligned} \quad (12)$$

where $\mathcal{S}_{A2} = \mathcal{S}_c(d, r_D, R_I) \cap \mathcal{S}_c(d, r_I + R_p, R_I)$. The expression for the region \mathcal{S}_{A2} is given in Appendix B. In the last step, we use the fact that the spatial distribution of primary transmitters in $\mathcal{S}_c(d, r_I + R_p, R_I) - \mathcal{S}_{A2}$ is independent with that in the r_D or $r_I + R_p$ circle of A and the R_I circle of B .

For $Pr\{k \text{ tx} \in \mathcal{S}_c(d, r_I + R_p, R_I) - \mathcal{S}_{A2}\}$, it is easy to see that

$$Pr\{k \text{ tx} \in \mathcal{S}_c(d, r_I + R_p, R_I) - \mathcal{S}_{A2}\} = \frac{(p(\lambda_{A1} - \lambda_{A2}^2))^k}{k!} \exp(-p(\lambda_{A1} - \lambda_{A2}^2)), \quad (13)$$

where $\lambda_{A2}^2 = \lambda\mathcal{S}_{A2}$.

Let $P_2 = Pr\{\overline{\mathbb{I}(A, r_I, \mathbf{rx})} \mid [\text{one tx} \in \mathcal{S}_c(d, r_I + R_p, R_I) - \mathcal{S}_{A2}] \cap \overline{\mathbb{I}(A, r_D, \mathbf{tx})} \cap \overline{\mathbb{I}(B, R_I, \mathbf{tx})}\}$, then we have that

$$\begin{aligned} & Pr\{\overline{\mathbb{I}(A, r_I, \mathbf{rx})} \mid [k \text{ tx} \in \mathcal{S}_c(d, r_I + R_p, R_I) - \mathcal{S}_{A2}] \cap \overline{\mathbb{I}(A, r_D, \mathbf{tx})} \cap \overline{\mathbb{I}(B, R_I, \mathbf{tx})}\} \\ &= P_2^k = \left(\iint_{\mathcal{S}_c(d, r_I + R_p, R_I) - \mathcal{S}_{A2}} \frac{1}{\mathcal{S}_c(d, r_I + R_p, R_I) - \mathcal{S}_{A2}} \left[1 - \frac{\mathcal{S}_I(r, R_p, r_I)}{\pi R_p^2} \right] r dr d\theta \right)^k \end{aligned} \quad (14)$$

$$\square P_F$$

Substitute (13), (14) into (12), and use the formula $\exp(x) = \sum_{k=0}^{\infty} \frac{x^k}{k!}$, and then substitute (8), (11) and (12) into (10),

$$\begin{aligned} P_F &= 1 - \exp[-p((\lambda_{A1} - \lambda_{A2}^2)(1 - P_2) + \lambda_{AB} - \lambda_{A1}(1 - P_1) - \lambda_B)], \\ &= 1 - \exp \left[-p\lambda \left(\pi r_D^2 - \mathcal{S}_I(d, r_D, R_I) - \iint_{\mathcal{S}_{A2}} \frac{\mathcal{S}_I(r, R_p, r_I)}{\pi R_p^2} r dr d\theta \right) \right]. \end{aligned} \quad (15)$$

2) *Miss Detection Probability* P_{MD} :

For LBT miss detection occurs if and only if the secondary transmitter A does not detect the presence of primary transmitters under \mathcal{H}_0 (see Fig. 6). We thus have

$$\begin{aligned} P_{MD} &= Pr\{\overline{\mathbb{I}(A, r_D, \text{tx})} \mid \mathcal{H}_1\}, \\ &= Pr\{\overline{\mathbb{I}(A, r_D, \text{tx})} \mid \mathbb{I}(A, r_I, \text{rx}) \cup \mathbb{I}(B, R_I, \text{tx})\}. \end{aligned} \quad (16)$$

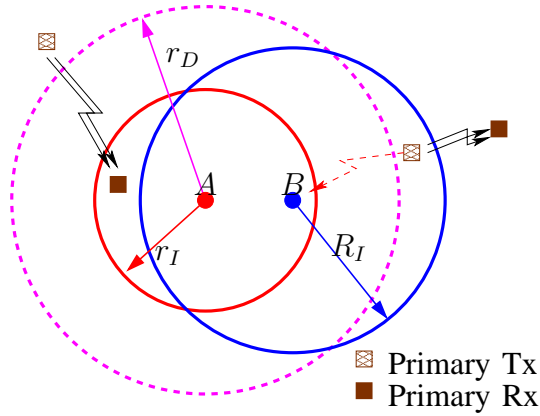


Fig. 6. An illustration of miss detection (Under \mathcal{H}_1 , there exists no primary tx within r_D of A)

In order to use our known results about false alarm probability P_F , we write P_{MD} as follows:

$$\begin{aligned} P_{MD} &= \frac{Pr\{\overline{\mathbb{I}(A, r_D, \text{tx})}\} - Pr\{\overline{\mathbb{I}(A, r_D, \text{tx})} \cap \overline{\mathbb{I}(A, r_I, \text{rx})} \cap \overline{\mathbb{I}(B, R_I, \text{tx})}\}}{Pr[\mathcal{H}_1]}, \\ &= \frac{Pr\{\overline{\mathbb{I}(A, r_D, \text{tx})}\} - Pr\{\overline{\mathbb{I}(A, r_D, \text{tx})} \cap \overline{\mathbb{I}(A, r_I, \text{rx})} \cap \overline{\mathbb{I}(B, R_I, \text{tx})}\}}{1 - Pr[\mathcal{H}_0]}. \end{aligned} \quad (17)$$

Since

$$Pr\{\overline{\mathbb{I}(A, r_D, \text{tx})}\} = \exp(-p\lambda_{A3}), \quad (18)$$

$$\begin{aligned} &Pr\{\overline{\mathbb{I}(A, r_D, \text{tx})} \cap \overline{\mathbb{I}(A, r_I, \text{rx})} \cap \overline{\mathbb{I}(B, R_I, \text{tx})}\} \\ &= Pr\{\overline{\mathbb{I}(A, r_I, \text{rx})} \mid \overline{\mathbb{I}(A, r_D, \text{tx})} \cap \overline{\mathbb{I}(B, R_I, \text{tx})}\} \cdot Pr\{\overline{\mathbb{I}(A, r_D, \text{tx})} \cap \overline{\mathbb{I}(B, R_I, \text{tx})}\}, \end{aligned} \quad (19)$$

where $\lambda_{A3} = \lambda\pi r_D^2$, it follow from (8), (11), and (12) that the expression for P_{MD} is obtained as below.

$$P_{MD} = \frac{\exp(-p\lambda\pi r_D^2) - \exp\left[-p\lambda\left(\pi(r_D^2 + R_I^2) - \mathcal{S}_I(d, r_D, R_I) + \iint_{\mathcal{S}_c(d, r_I+R_p, R_I)-\mathcal{S}_{A2}} \frac{\mathcal{S}_I(r, R_p, r_I)}{\pi R_p^2} r dr d\theta\right)\right]}{1 - \exp\left[-p\lambda\left(\iint_{\mathcal{S}_c(d, r_I+R_p, R_I)} \frac{\mathcal{S}_I(r, R_p, r_I)}{\pi R_p^2} r dr d\theta + \pi R_I^2\right)\right]} \quad (20)$$

3) *Properties:*

□ **Property 1** For fixed $p\lambda$, r_I , d , R_I , and R_p , $P_F \uparrow$ and $P_{MD} \downarrow$ as $r_D \uparrow$.

Proof. Since

$$\pi r_D^2 - \mathcal{S}_I(d, r_D, R_I) - \iint_{\mathcal{S}_{A2}} \frac{\mathcal{S}_I(r, R_p, r_I)}{\pi R_p^2} r dr d\theta = \iint_{\mathcal{S}_{A2}} \left[1 - \frac{\mathcal{S}_I(r, R_p, r_I)}{\pi R_p^2}\right] r dr d\theta$$

and the area \mathcal{S}_{A2} of the double integral increases as r_D increases, it follows from the monotonicity of exponential function that P_F is an increasing function of r_D .

On the other hand, since

$$P_{MD} = \frac{\exp(-p\lambda\pi r_D^2) \left\{1 - \exp\left[-p\lambda\left(\pi R_I^2 - \mathcal{S}_I(d, r_D, R_I) + \iint_{\mathcal{S}_c(d, r_I+R_p, R_I)-\mathcal{S}_{A2}} \frac{\mathcal{S}_I(r, R_p, r_I)}{\pi R_p^2} r dr d\theta\right)\right]\right\}}{1 - \exp\left[-p\lambda\left(\iint_{\mathcal{S}_c(d, r_I+R_p, R_I)} \frac{\mathcal{S}_I(r, R_p, r_I)}{\pi R_p^2} r dr d\theta + \pi R_I^2\right)\right]}$$

by considering the monotonicity of $\exp(-p\lambda\pi r_D^2)$, $\mathcal{S}_I(d, r_D, R_I)$, and \mathcal{S}_{A2} with respect to r_D , we conclude that P_{MD} is a decreasing function of r_D . □

□ **Property 2** For fixed r_D , r_I , d , R_I , and R_p , $P_F \uparrow$ as $p\lambda \uparrow$.

Proof. Since from the definition of \mathcal{S}_{A2} , we know that πr_D^2 is always larger than or equal to $\mathcal{S}_I(d, r_D, R_I) + \iint_{\mathcal{S}_{A2}} \frac{\mathcal{S}_I(r, R_p, r_I)}{\pi R_p^2} r dr d\theta$, based on the monotonicity of exponential function, we can conclude that $P_F \uparrow$ as $p\lambda \uparrow$ given other parameters. □

□ **Property 3** For fixed r_D , r_I , d , R_I , and R_p , $P_{MD} \downarrow$ as $p\lambda \uparrow$.

Proof. Let

$$\begin{aligned}
 u &= p\lambda \\
 s_1 &= \pi r_D^2 \\
 s_2 &= \pi R_I^2 - \mathcal{S}_I(d, r_D, R_I) + \iint_{\mathcal{S}_c(d, r_I + R_p, R_I) - \mathcal{S}_{A2}} \frac{\mathcal{S}_I(r, R_p, r_I)}{\pi R_p^2} r dr d\theta \\
 s_3 &= \iint_{\mathcal{S}_c(d, r_I + R_p, R_I)} \frac{\mathcal{S}_I(r, R_p, r_I)}{\pi R_p^2} r dr d\theta + \pi R_I^2
 \end{aligned}$$

and by recalling the definition of $\mathcal{S}_c(d, r_I + R_p, R_I)$ and \mathcal{S}_{A2} , we can easily find that u , s_1 , s_2 , and s_3 satisfy the following properties: all of them are positive, and $s_1 + s_2 \geq s_3$, $s_2 \leq s_3$. Then we only need to show the function

$$f(u) = \frac{\exp(-us_1)(1 - \exp(-us_2))}{1 - \exp(-us_3)}$$

is a decreasing function of u ($u > 0$) with $s_1, s_2, s_3 > 0$ and $s_1 + s_2 \geq s_3$, $s_2 < s_3^2$.

By replacing $\exp(-u)$ by x ($0 < x < 1$), we obtain a new function of x .

$$g(x) = \frac{x^{s_1}(1 - x^{s_2})}{1 - x^{s_3}} = x^{s_1 - (s_3 - s_2)} \cdot \frac{x^{s_3 - s_2} - x^{s_3}}{1 - x^{s_3}}$$

Since $x = \exp(-u)$ is monotonically decreasing and $x^{s_1 - (s_3 - s_2)}$ ($s_1 - (s_3 - s_2) \geq 0$) is monotonically increasing, it is equivalent to show that $h(x) = \frac{x^{s_3 - s_2} - x^{s_3}}{1 - x^{s_3}}$ is an increasing function of x for $0 < x < 1$.

Take the derivative of $h(x)$,

$$h'(x) = \frac{x^{s_3 - s_2 - 1} [s_3(1 - x^{s_2}) - s_2(1 - x^{s_3})]}{(1 - x^{s_3})^2}$$

Next we will show that $s_3(1 - x^{s_2}) - s_2(1 - x^{s_3}) \geq 0$, *i.e.*, $\frac{1 - x^{s_2}}{s_2} \geq \frac{1 - x^{s_3}}{s_3}$ for $0 < s_2 < s_3$.

To prove this inequality, we define a function of a

$$p(a) = \frac{1 - x^a}{a} \quad (0 < x < 1).$$

Take the derivative with respect to a ,

$$p'(a) = \frac{-(\ln(x))x^a a - (1 - x^a)}{a^2}$$

²If $s_2 = s_3$, then $f(u) = \exp(-us_1)$ and the proof is trivial

Denote the numerator of $p'(a)$ by $q(a)$, then we have that

$$\begin{aligned} q(0) &= 0, \quad q'(a) = -(\ln(x))^2 x^a a < 0, \quad \text{for all } a > 0 \\ \Rightarrow q(a) &< 0, \quad \text{for all } a > 0, \quad \text{i.e., } p'(a) < 0, \quad \text{for all } a > 0 \end{aligned}$$

So $p(a)$ is monotonically decreasing with respect to a . It follows that the inequality holds for $0 < s_2 < s_3$. Hence, $h(x)$ is an increasing function of x ($0 < x < 1$). \square

C. MAC Performance

1) Collision Probability P_C :

Since the secondary transmitter A transmits data if and only if A detects no nearby primary transmitters (see Fig. 7), by recalling (1), we have

$$P_C = Pr\{\overline{\mathbb{I}(A, r_D, \text{tx})} \mid \mathbb{I}(A, r_I, \text{rx})\}. \quad (21)$$

Note that collision probability P_C does not depend on the activities of primary users near the secondary receiver B . Moreover, By comparing (21) with (16), we can easily see that $P_C \neq P_{MD}$.

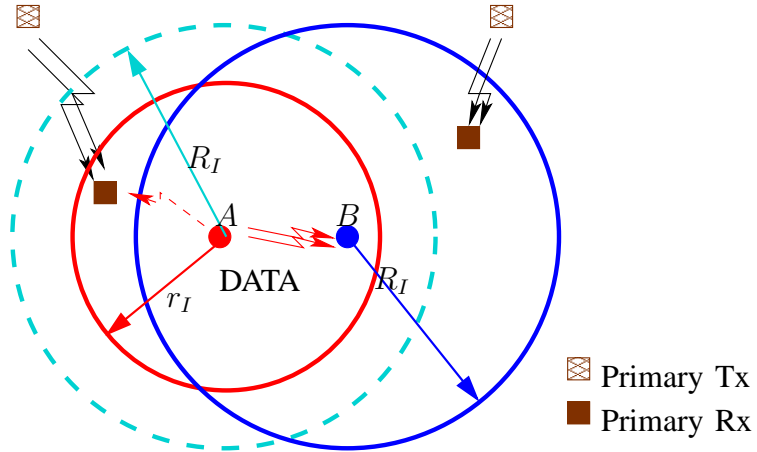


Fig. 7. An illustration of collision (there exists no tx within r_D of $A \Rightarrow$ Collision with some rx within r_I of A)

Based on the basic property of conditional probability, we have that

$$P_C = \frac{Pr\{\overline{\mathbb{I}(A, r_D, \text{tx})} \cap \mathbb{I}(A, r_I, \text{rx})\}}{Pr\{\mathbb{I}(A, r_I, \text{rx})\}}. \quad (22)$$

Since according to the Displacement Theorem primary receivers admits a spatial Poisson distribution with density $p\lambda$, it follows that

$$Pr\{\mathbb{I}(A, r_I, \mathbf{rx})\} = 1 - \exp(-p\lambda\pi r_I^2). \quad (23)$$

Then by using the similar techniques in the derivation of the expression for $Pr[\mathcal{H}_0]$, we can obtain the expression for the probability in the numerator of (22). So collision probability P_C is given by

$$P_C = \frac{\exp(-p\lambda\pi r_D^2)[1 - \exp(-p\lambda\pi(r_I^2 - I(r_D, r_I, R_p)))]}{1 - \exp(-p\lambda\pi r_I^2)}, \quad (24)$$

where $I(r_D, r_I, R_p) = \int_0^{r_D} 2r \frac{S_I(r, r_I, R_p)}{\pi R_p^2} dr$. If we substitute the expression for $S_I(r, r_I, R_p)$ into the above integral, we can actually obtain a closed-form expression for $I(r_D, r_I, R_p)$ (see Appendix C).

2) Successful Transmission Probability P_S :

For applications with guaranteed delivery, an acknowledgement (ACK) signal from B to the secondary transmitter A is required to complete a data transmission. In this case successful data transmission occurs if and only if the ACK signal is successfully received at A . But since spectrum opportunity is asymmetric (see Sec. III), correctly identified opportunity may not lead to a successful transmission (see Fig. 8). On the other hand, as shown in Fig. 9, if there are some primary receivers within r_I of A , but no primary transmitters within R_I of A and B , then miss detection leads to a successful transmission.

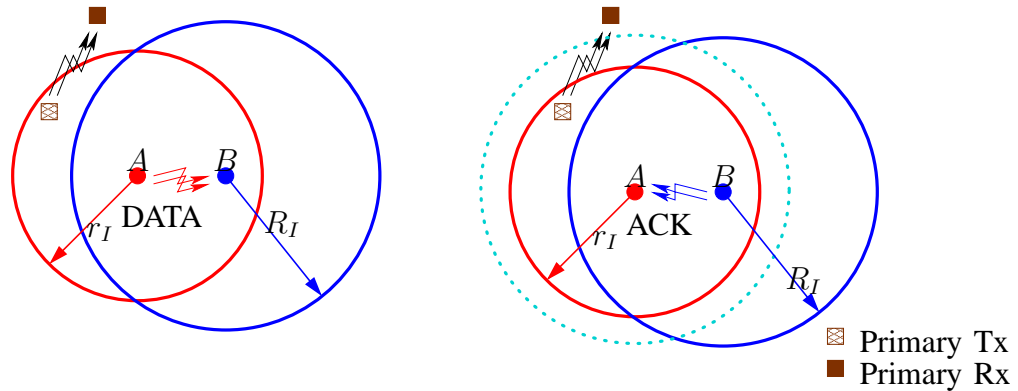


Fig. 8. Successful data transmission but failed ACK

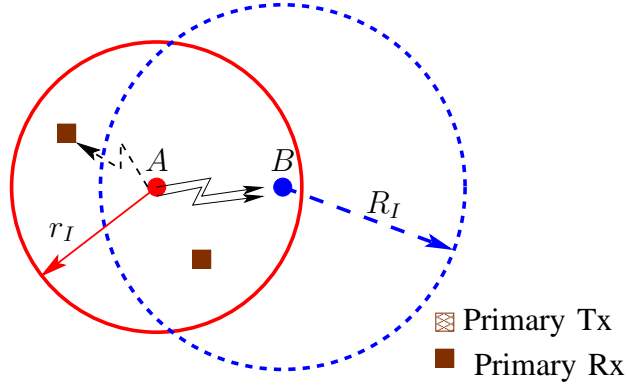


Fig. 9. Miss detection leads to successful transmission.

Let the effective range $r_E = \max\{r_D, R_I\}$, then followed from the above facts, we can express the probability P_S of successful data transmission as follows:

$$\begin{aligned}
 P_S &= Pr\{\text{successful data transmission}\}, \\
 &= Pr\{\text{successful transmission} \mid \mathcal{H}_0\} \cdot Pr[\mathcal{H}_0] + Pr\{\text{successful transmission} \mid \mathcal{H}_1\} \cdot Pr[\mathcal{H}_1], \\
 &= Pr[\overline{\mathbb{I}(A, r_E, \text{tx})} \mid \mathcal{H}_0] \cdot Pr[\mathcal{H}_0] + Pr[\overline{\mathbb{I}(A, r_E, \text{tx})} \cap \overline{\mathbb{I}(B, R_I, \text{tx})} \mid \mathcal{H}_1] \cdot Pr[\mathcal{H}_1]. \quad (25)
 \end{aligned}$$

By comparing (25) with (9) and (16), we can easily see that

$$\begin{aligned}
 Pr\{\text{successful transmission} \mid \mathcal{H}_0\} &\leq 1 - P_F, \\
 Pr\{\text{successful transmission} \mid \mathcal{H}_1\} &\leq P_{MD}.
 \end{aligned}$$

By using the definition of \mathcal{H}_0 and \mathcal{H}_1 , we can simplify the expression for P_S into the following form:

$$\begin{aligned}
 P_S &= Pr\{\overline{\mathbb{I}(A, r_E, \text{tx})} \cap \overline{\mathbb{I}(B, R_I, \text{tx})}\}, \\
 &= \exp[-p\lambda(\pi(r_E^2 + R_I^2) - \mathcal{S}_I(d, r_E, R_I))]. \quad (26)
 \end{aligned}$$

From (26), it seems that the success probability P_S does not depend on r_I . But since the collision probability P_C (see (24)) depends on r_I , and there is a constraint on P_C ($P_C \leq \zeta$), it follows that given different r_I , r_D probably needs to be chosen differently to meet the constraint on P_C and therefore it results in different P_S .

We now consider the success probability P_S for applications relying on best-effort delivery (for example, media streaming and network gaming). For these applications, ACKs are not

necessary. Since ACK is not involved in opportunity detection and collision with primary users, given the same parameters (p , λ , R_p , R_I , d , r_I , and r_D) we have the same expressions for false alarm probability P_F , miss detection probability P_{MD} , and collision probability P_C as before but different successful transmission probability P_S .

For best-effort delivery, data transmission is successful if and only if data is received successfully at the secondary receiver B . So the probability P_S of successful data transmission is given by

$$\begin{aligned}
 P_S &= Pr\{\text{successful data transmission}\}, \\
 &= Pr\{\text{successful transmission} \mid \mathcal{H}_0\} \cdot Pr[\mathcal{H}_0] + Pr\{\text{successful transmission} \mid \mathcal{H}_1\} \cdot Pr[\mathcal{H}_1], \\
 &= Pr[\overline{\mathbb{I}(A, r_D, \text{tx})} \mid \mathcal{H}_0] \cdot Pr[\mathcal{H}_0] + Pr[\overline{\mathbb{I}(A, r_D, \text{tx})} \cap \overline{\mathbb{I}(B, R_I, \text{tx})} \mid \mathcal{H}_1] \cdot Pr[\mathcal{H}_1], \\
 &= Pr\{\overline{\mathbb{I}(A, r_D, \text{tx})} \cap \overline{\mathbb{I}(B, R_I, \text{tx})}\}, \\
 &= \exp[-p\lambda(\pi(r_D^2 + R_I^2) - \mathcal{S}_I(d, r_D, R_I))]. \tag{27}
 \end{aligned}$$

By comparing (27) with (9) and (16), we can easily see that for best-effort delivery:

$$\begin{aligned}
 Pr\{\text{successful transmission} \mid \mathcal{H}_0\} &= 1 - P_F, \\
 Pr\{\text{successful transmission} \mid \mathcal{H}_1\} &\leq P_{MD}.
 \end{aligned}$$

D. Performance of RTS/CTS enhanced LBT

The fundamental deficiency of LBT resembles the hidden and exposed terminal problem in the conventional ad hoc networks of peer users. It is thus natural to consider the use of RTS/CTS handshaking signaling to enhance the detection performance of LBT.

For RTS/CTS enhanced LBT, spectrum opportunity detection is performed jointly by the secondary transmitter A and the secondary receiver B through the exchange of RTS/CTS signals. The detailed steps of RTS/CTS enhanced LBT is listed as below.

- A detects primary transmitters within distance r_D . If it detects none, A sends B a Ready-to-Send (RTS) signal.
- If B receives the RTS signal from A successfully, which automatically indicates the absence of primary transmitters within distance R_I , then B replies with a Clear-to-Send (CTS) signal.
- Upon receiving the CTS signal, A transmits data to B .

Then we will derive the expressions for false alarm probability P_F , miss detection probability P_{MD} , collision probability P_C , and successful transmission probability P_S one by one.

1) *False Alarm Probability P_F :*

For RTS/CTS enhanced LBT, the observation space of opportunity detection comprises the RTS and CTS signals. So false alarm occurs if and only if the RTS/CTS exchange fails under \mathcal{H}_0 (see Fig. 10 and Fig. 11). It follows that false alarm probability P_F is given by

$$P_F = Pr\{\mathbb{I}(A, r_E, \text{tx}) \mid \mathcal{H}_0\} \quad (28)$$

By comparing (28) with (9), we find that they are almost the same except that r_D is replaced by r_E in (28). Hence we have that

$$P_F = 1 - \exp \left[-p\lambda \left(\pi r_E^2 - \mathcal{S}_I(d, r_E, R_I) - \iint_{\mathcal{S}_{A1}} \frac{\mathcal{S}_I(r, R_p, r_I)}{\pi R_p^2} r dr d\theta \right) \right], \quad (29)$$

where $\mathcal{S}_{A1} = \mathcal{S}_c(d, r_E, R_I) \cap \mathcal{S}_c(d, r_I + R_p, R_I)$, and the detailed form of \mathcal{S}_{A1} can be found in Appendix B.

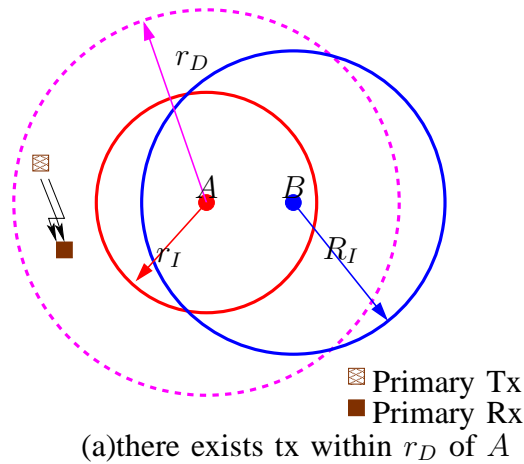


Fig. 10. Case 1: A detects primary transmitter.

2) *Miss Detection Probability P_{MD} :*

For RTS/CTS enhanced LBT, miss detection occurs if and only if the RTS/CTS exchange is successful under \mathcal{H}_1 (see Fig. 12). So miss detection probability P_{MD} is given by

$$P_{MD} = Pr\{\overline{\mathbb{I}(A, r_D, \text{tx})} \cap \overline{\mathbb{I}(B, R_I, \text{tx})} \cap \overline{\mathbb{I}(A, R_I, \text{tx})} \mid \mathcal{H}_1\}. \quad (30)$$

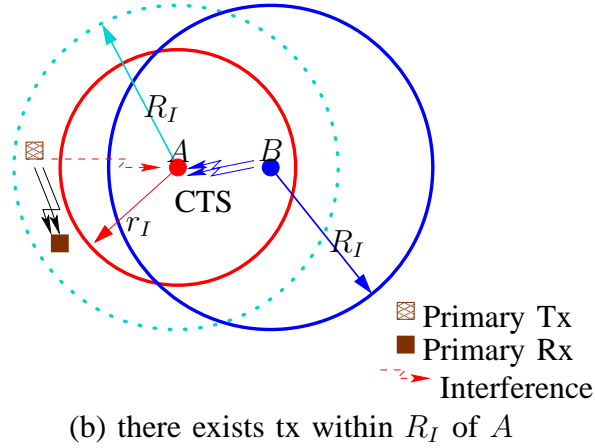


Fig. 11. Case 2: A fails to receive CTS.

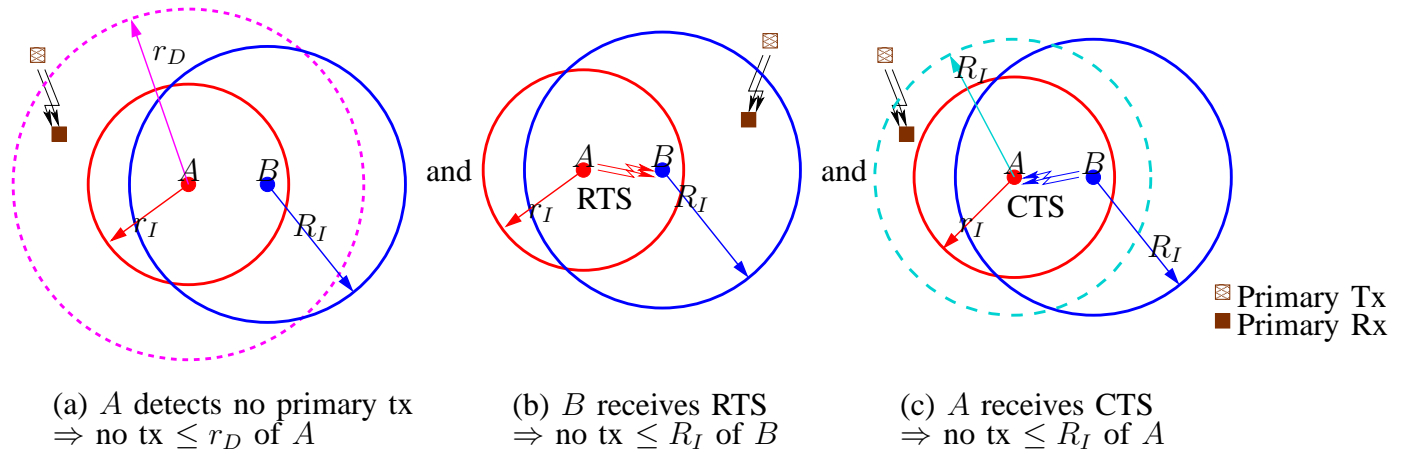


Fig. 12. An illustration of miss detection

Then by using Bayes rule, we can express (30) in the form of some know probabilities.

$$\begin{aligned}
 P_{MD} &= \frac{\Pr\{\overline{\mathbb{I}(A, r_E, \text{tx})} \cap \mathbb{I}(A, r_I, \text{rx}) \cap \overline{\mathbb{I}(B, R_I, \text{tx})}\}}{\Pr[\mathcal{H}_1]}, \\
 &= \frac{\left(1 - \Pr\{\overline{\mathbb{I}(A, r_I, \text{rx})} \mid \mathbb{I}(A, r_E, \text{tx}) \cap \overline{\mathbb{I}(B, R_I, \text{tx})}\}\right) \cdot \Pr\{\overline{\mathbb{I}(A, r_E, \text{tx})} \cap \overline{\mathbb{I}(B, R_I, \text{tx})}\}}{1 - \Pr[\mathcal{H}_0]}. \quad (31)
 \end{aligned}$$

By recalling (8), (11), and (12), we have that

$$\begin{aligned}
 P_{MD} &= \frac{\exp(-p\lambda_{AB})[1 - \exp(-p(\lambda_{A1} - \lambda_{A2}^1)(1 - P_2))]}{1 - \exp[-p(\lambda_{A1}(1 - P_1) + \lambda_B)]}, \\
 &= \frac{\exp[-p\lambda(\pi(r_E^2 + R_I^2) - \mathcal{S}_I(d, r_E, R_I))] \left[1 - \exp\left(-p\lambda \iint_{\mathcal{S}_c(d, r_I + R_p, R_I) - \mathcal{S}_{A1}} \frac{\mathcal{S}_I(r, R_p, r_I)}{\pi R_p^2} r dr d\theta\right) \right]}{1 - \exp\left[-p\lambda \left(\iint_{\mathcal{S}_c(d, r_I + R_p, R_I)} \frac{\mathcal{S}_I(r, R_p, r_I)}{\pi R_p^2} r dr d\theta + \pi R_I^2 \right) \right]} \quad (32)
 \end{aligned}$$

where $\lambda_{A2}^1 = \lambda \mathcal{S}_{A1}$.

3) Collision Probability P_C :

For RTS/CTS enhanced LBT, given that there exists some primary receiver within the interference range r_I of the secondary transmitter A , collision occurs if and only if the RTS/CTS exchange is successful (see Fig. 13). So collision probability P_C is given by

$$P_C = Pr\{\overline{\mathbb{I}(A, r_E, \text{tx})} \cap \overline{\mathbb{I}(B, R_I, \text{tx})} \mid \mathbb{I}(A, r_I, \text{rx})\}. \quad (33)$$

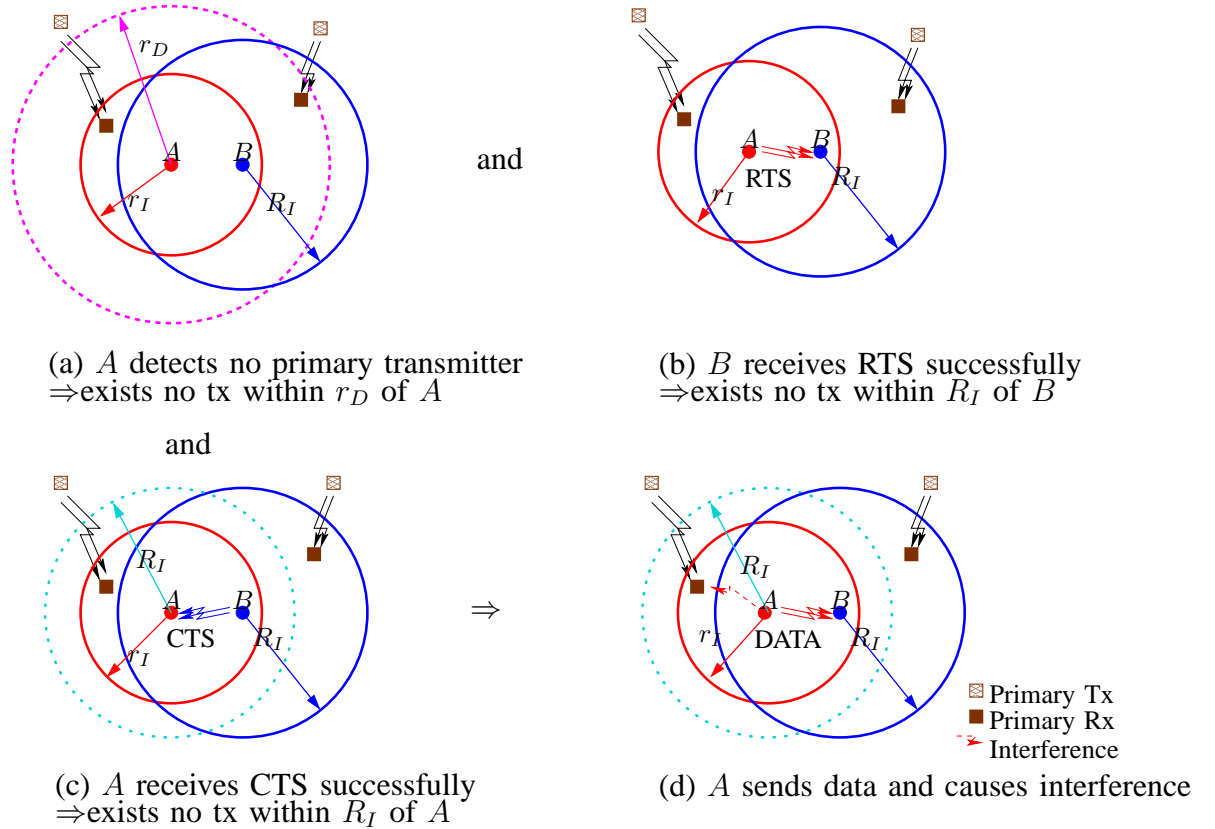


Fig. 13. An illustration of collision

By comparing (33) with (16), we have that

$$\begin{aligned}
 P_C &= \frac{Pr[\mathcal{H}_1]}{Pr\{\mathbb{I}(A, r_I, \text{rx})\}} P_{MD}, \\
 &= \frac{\exp[-p\lambda(\pi(r_E^2 + R_I^2) - \mathcal{S}_I(d, r_E, R_I))] \left[1 - \exp\left(-p\lambda \iint_{\mathcal{S}_c(d, r_I + R_p, R_I) - \mathcal{S}_{A1}} \frac{\mathcal{S}_I(r, R_p, r_I)}{\pi R_p^2} r dr d\theta\right) \right]}{1 - \exp(p\lambda\pi r_I^2)} \quad (34)
 \end{aligned}$$

Note that $Pr[\mathcal{H}_1] = Pr\{\mathbb{I}(A, r_I, \text{rx}) \cup \mathbb{I}(B, R_I, \text{tx})\} \geq Pr\{\mathbb{I}(A, r_I, \text{rx})\}$, so $P_C \geq P_{MD}$.

4) Successful Transmission Probability P_S :

For RTS/CTS enhanced LBT, a data transmission is successful if and only if the RTS/CTS exchange is successful (see Fig. 14). The secondary transmitter A sends data to the secondary receiver B only if A receives CTS from B . Since before B replies with CTS B must receive RTS successfully, B can also receive data successfully. So the probability P_S of successful data transmission is given by

$$\begin{aligned}
 P_S &= Pr\{\overline{\mathbb{I}(A, r_E, \text{tx})} \cap \overline{\mathbb{I}(B, R_I, \text{tx})}\}, \\
 &= \exp[-p\lambda(\pi(r_E^2 + R_I^2) - \mathcal{S}_I(d, r_E, R_I))]. \quad (35)
 \end{aligned}$$

Notice that P_S of RTS/CTS enhanced LBT is identical to that of LBT without RTS/CTS for guaranteed delivery in (27). Moreover, using RTS/CTS enhanced LBT, the throughput is the same for guaranteed delivery and best-effort delivery.

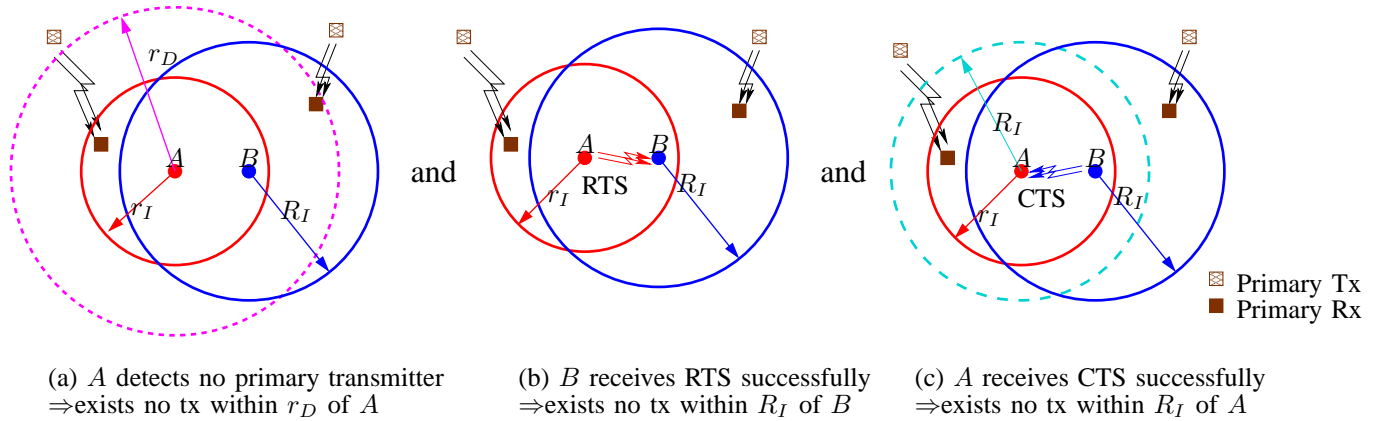


Fig. 14. An illustration of successful transmission

5) *Properties*: By using techniques similar to proving these properties for LBT, we can show that Property 1,2,3,4 also hold for RTS/CTS enhanced LBT.

VI. NUMERICAL EXAMPLES

In this section, we first study the PHY layer performance of opportunity detection for LBT by observing the ROC curves, and then we investigate the impact of application and MAC handshaking signaling on the translation from PHY layer performance to MAC layer performance. All the figures in this section are plotted based on the expressions derived in Sec. V.

A. PHY Performance

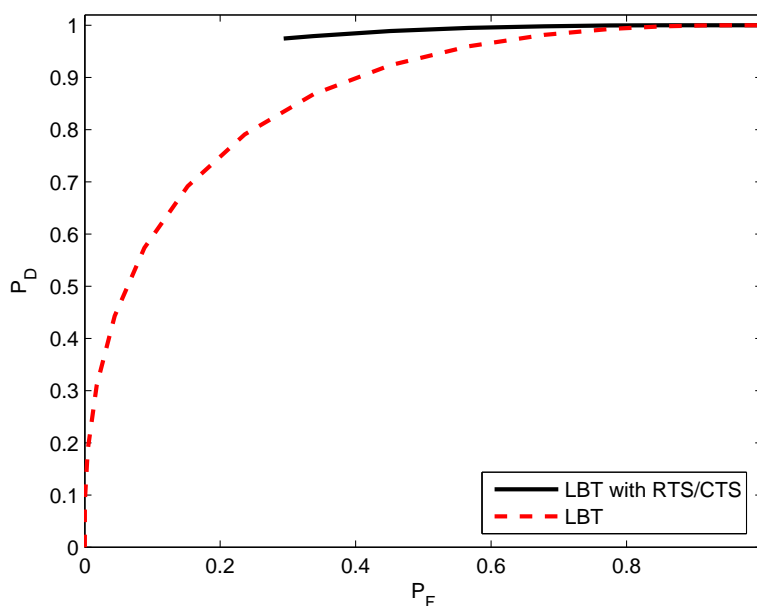


Fig. 15. ROC performance comparison ($p = 0.03$, $\lambda = 10/200^2$, $R_p = 200m$, $R_I = 250m$, $d = 200m$, $r_I = 200m/0.9$).

In Fig. 15, we plot the ROC curves for both LBT and RTS/CTS enhanced LBT, and we can observe the following facts:

- $(0,0)$ does not belong to the ROC curve of RTS/CTS enhanced LBT. This is due to the fact that the effective detection range is bounded above R_I , since to receive the CTS signal successfully, there cannot be primary transmitters within R_I of A . In other words, a detection range $r_D \leq R_I$ leads to the same (P_F, P_{MD}) as $r_D = R_I$.
- The ROC performance of RTS/CTS enhanced LBT is always better than or equal to that of LBT when $r_D \geq R_I$. When $r_D < R_I$, we can use randomized detection with parameter p_T

to complete the irregular ROC curve of RTS/CTS enhanced LBT in this range. Specifically, if the RTS/CTS exchange succeeds, we decide \mathcal{H}_0 ; otherwise, if the RTS/CTS exchange fails, we decide \mathcal{H}_0 with probability p_T and \mathcal{H}_1 with probability $1 - p_T$. In this case, there is a straight line that connects $(0,0)$ with the point (P_F, P_D) where $r_D = R_I$, *i.e.*, the starting point in Fig. 15. It is easy to see that in this range, the ROC performance of this randomized LBT with RTS/CTS may be worse than that of LBT.

B. Impact of Application

Since the design objective is to maximize P_S (representing link throughput) under a collision constraint $P_C \leq \zeta$, we show P_S as a function of P_C in Fig. 16.

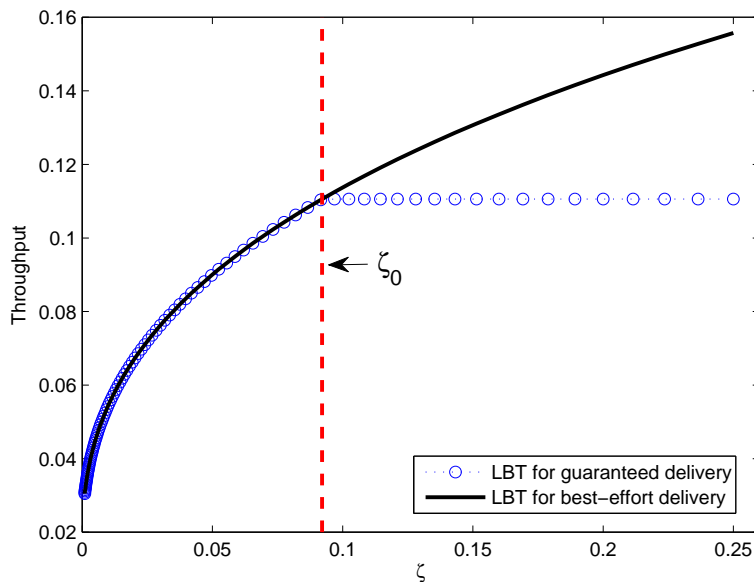


Fig. 16. Success probability vs interference constraint ($p = 0.03$, $\lambda = 10/200^2$, $R_p = 200m$, $R_I = 250m$, $d = 200m$, $r_I = 200m/0.9$).

From Fig. 16, we observe that even though the detection performance at the physical layer is the same (see Fig. 15), the MAC layer performance can be different depending on the applications. When the collision constraint is tight, the throughput is the same for these two types of applications. The collision constraint ζ has a critical value ζ_0 above which the throughput for best-effort delivery is higher than that for guaranteed delivery. Fig. 17 shows ζ_0 as a function

of the primary traffic load $p\lambda$ (or the density of active primary transmitters). We can see that ζ_0 is a decreasing function of $p\lambda$. This suggests that primary systems with heavy traffic is more suitable for spectrum overlay with best-effort delivery applications.

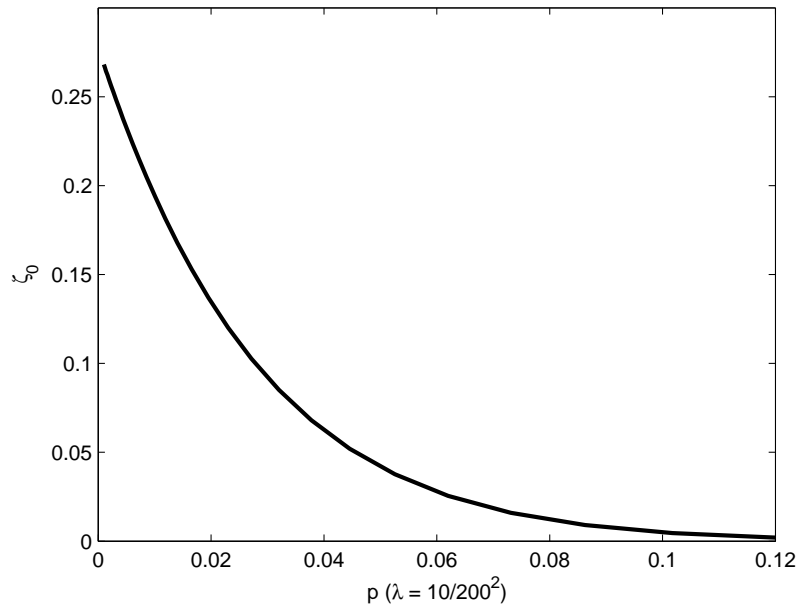


Fig. 17. Critical value of ζ vs. primary traffic load ($\lambda = 10/200^2$, $R_p = 200m$, $r_D = R_I = 250m$, $d = 200m$, $r_I = 200m/0.9$).

C. Impact of MAC Handshaking Signaling

Fig. 18 shows P_S as a function of P_C for LBT in two typical applications (guaranteed delivery, best-effort delivery) and RTS/CTS enhanced LBT. Note that using RTS/CTS enhanced LBT, the throughput is the same for guaranteed delivery and best-effort delivery. We can see that at the RTS/CTS enhanced LBT may lead to lower throughput when the collision constraint is loose and the application relies on best-effort delivery. Note that even random detection is used in RTS/CTS enhanced LBT for $r_D < R_I$ to complete the ROC curve, its throughput can still be lower than that of LBT for best-effort delivery when ζ is relatively large as shown in Fig. 19.

VII. CONCLUSION

In this report, by considering a Poisson distributed primary network, we have derived the analytical expressions for opportunity detection performance at both PHY and MAC layers.

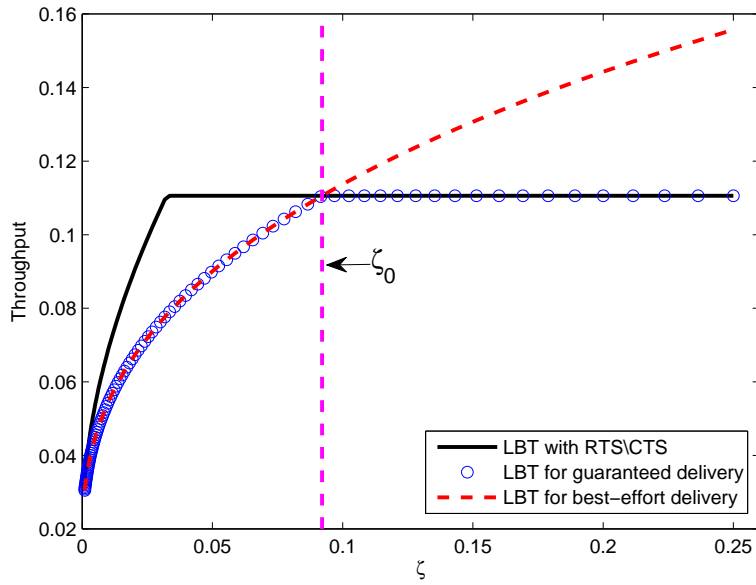


Fig. 18. Throughput comparison ($p = 0.03$, $\lambda = 10/200^2$, $R_p = 200m$, $R_I = 250m$, $d = 200m$, $r_I = 200m/0.9$).

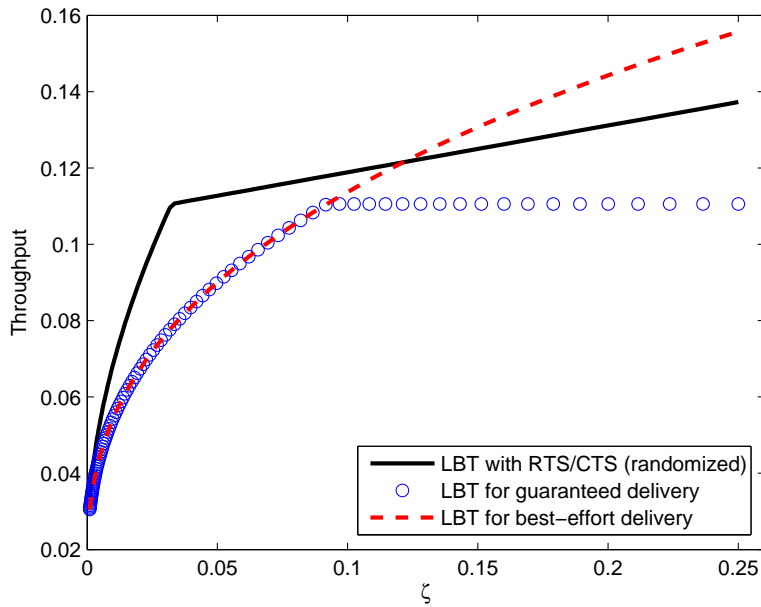


Fig. 19. Throughput comparison ($p = 0.03$, $\lambda = 10/200^2$, $R_p = 200m$, $R_I = 250m$, $d = 200m$, $r_I = 200m/0.9$).

Based on these expressions, we illustrate the complex dependency of the relationship between PHY and MAC on the application type (guaranteed delivery vs. best-effort delivery) and the use of handshaking signaling such as RTS/CTS at the MAC layer by some numerical examples. Specifically, when the interference constraint is tight, we should adopt RTS/CTS handshaking to improve the link throughput, but RTS/CTS handshaking leads to decreased throughput when the interference constraint is loose. Moreover, in primary networks with relatively heavy traffic best-effort delivery applications are more suitable than guaranteed delivery applications.

APPENDIX

A. Intersecting Area S_I of Two Circles

Assume that the radii of two circles are r_1 and r_2 respectively and the distance between the centers of two circles is d . Without loss of generality, we also assume that $r_2 > r_1$. The expression for S_I depends on the relation between d and $r_2 - r_1$, $r_1 + r_2$ (see Fig. 20), and it is given in the following three cases.

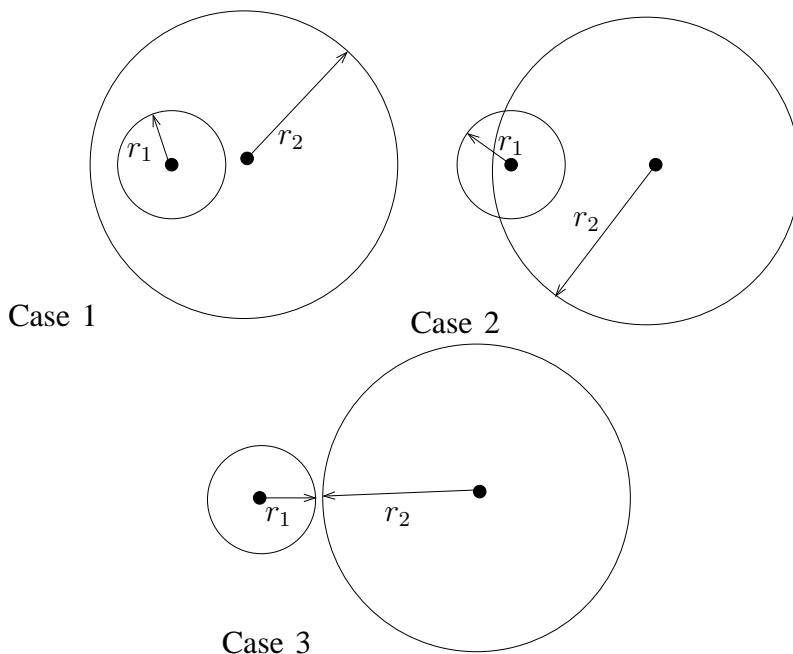


Fig. 20. Intersecting area of two circles

□ **Case 1** ($0 \leq d \leq r_2 - r_1$):

$$S_I(d, r_1, r_2) = \pi r_1^2$$

□ **Case 2** ($r_2 - r_1 < d < r_1 + r_2$) [4]:

$$\begin{aligned} \mathcal{S}_I(d, r_1, r_2) = & r_2^2 \cos^{-1} \left(\frac{r_2^2 + d^2 - r_1^2}{2 d r_2} \right) + r_1^2 \cos^{-1} \left(\frac{r_1^2 + d^2 - r_2^2}{2 d r_1} \right) \\ & - d \sqrt{r_1^2 - \left(\frac{r_1^2 + d^2 - r_2^2}{2 d} \right)^2} \end{aligned}$$

□ **Case 3** ($d \geq r_1 + r_2$):

$$\mathcal{S}_I(d, r_1, r_2) = 0$$

B. $\mathcal{S}_c(d, r_I + R_p, R_I)$, \mathcal{S}_{A1} and \mathcal{S}_{A2} in the Polar Coordinate System

Here we pick the secondary transmitter A as the origin.

1) $\mathcal{S}_c(d, r_I + R_p, R_I)$ – the area within a circle with radius $r_I + R_p$ centered at A but outside the circle with radius R_I centered at B :

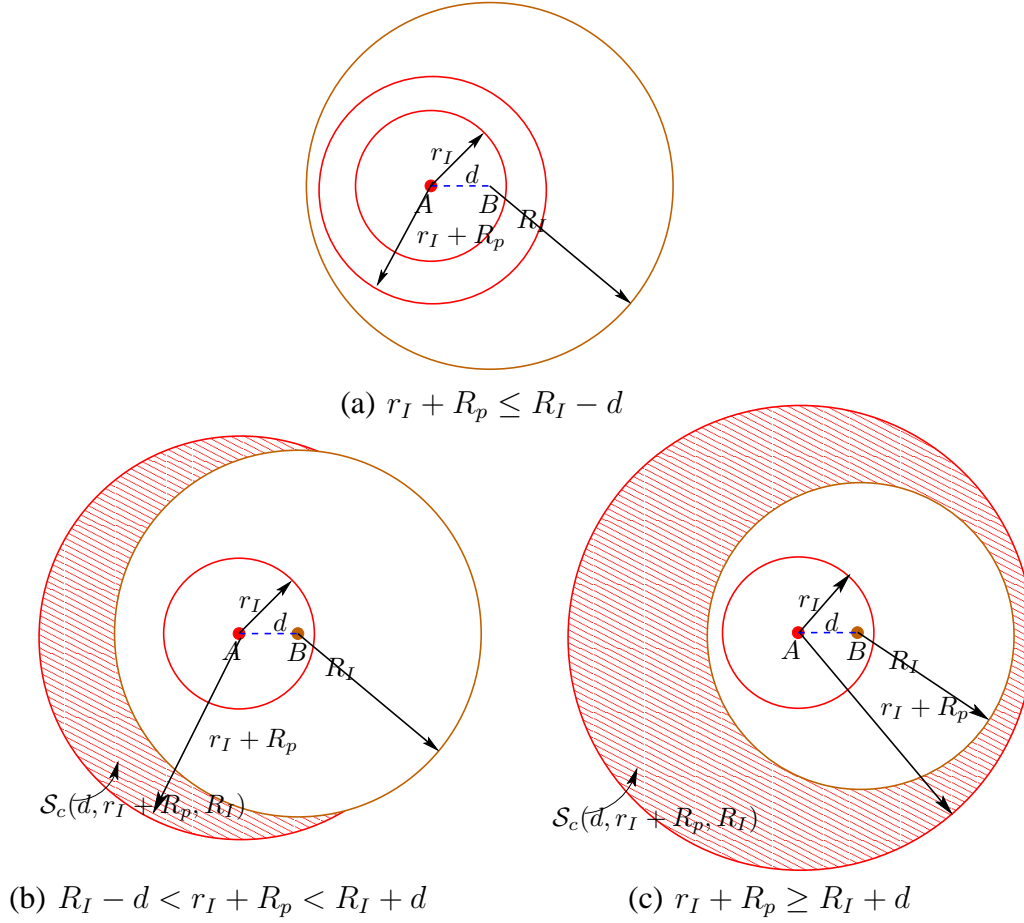
▷ **Case 1:** $R_I \geq d$ (see Fig. 21)

$$\begin{aligned} & \mathcal{S}_c(d, r_I + R_p, R_I) \\ = & \begin{cases} \phi, & \text{if } r_I + R_p \leq R_I - d, \\ R_I - d \leq r \leq r_I + R_p, \theta_0(r) \leq \theta(r) \leq 2\pi - \theta_0(r), & \text{if } R_I - d < r_I + R_p < R_I + d, \\ R_I - d \leq r \leq r_I + R_p, \begin{cases} \theta_0(r) \leq \theta(r) \leq 2\pi - \theta_0(r), & \text{for } r < R_I + d \\ 0 \leq \theta(r) < 2\pi, & \text{otherwise} \end{cases}, & \text{if } r_I + R_p \geq R_I + d, \end{cases} \end{aligned}$$

where $\theta_0(r) = \arccos \left(\frac{d^2 + r^2 - R_I^2}{2dr} \right)$.

▷ **Case 2:** $R_I < d$

$$\begin{aligned} & \mathcal{S}_c(d, r_I + R_p, R_I) \\ = & \begin{cases} 0 \leq r \leq r_I + R_p, 0 \leq \theta < 2\pi & \text{if } r_I + R_p \leq d - R_I, \\ 0 \leq r \leq r_I + R_p, \begin{cases} 0 \leq \theta(r) \leq 2\pi, & \text{for } r \leq d - R_I \\ \theta_0(r) \leq \theta(r) < 2\pi - \theta_0(r), & \text{otherwise} \end{cases}, & \text{if } d - R_I < r_I + R_p < R_I + d, \\ 0 \leq r \leq r_I + R_p, \begin{cases} \theta_0(r) \leq \theta(r) \leq 2\pi - \theta_0(r), & \text{for } d - R_I < r < R_I + d \\ 0 \leq \theta(r) < 2\pi, & \text{otherwise} \end{cases}, & \text{if } r_I + R_p \geq R_I + d. \end{cases} \end{aligned}$$


 Fig. 21. Illustration of \mathcal{S}_c (Case 1)

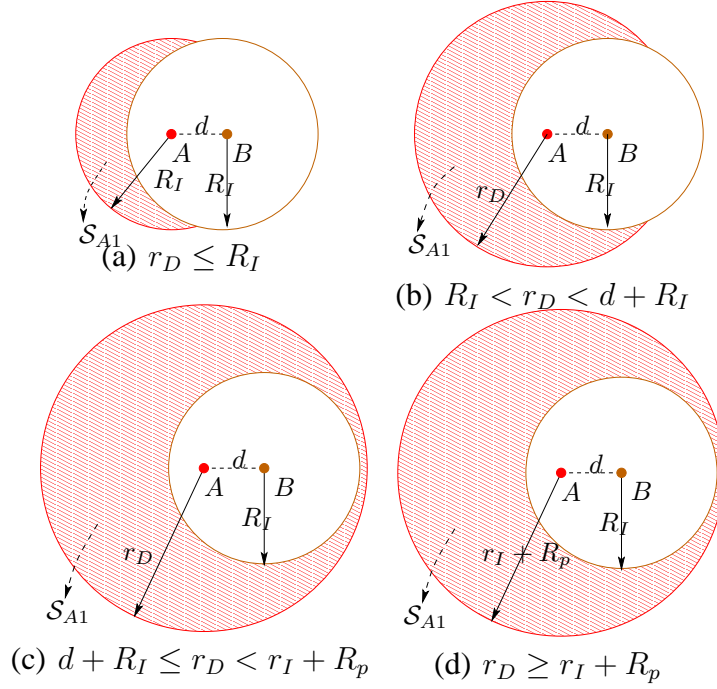
2) $\mathcal{S}_{A1} = \mathcal{S}_c(d, r_E, R_I) \cap \mathcal{S}_c(d, r_I + R_p, R_I)$:

▷ **Case 1:** $R_I \geq d$, $d + R_I < r_I + R_p$ (see Fig. 22)

$$\mathcal{S}_{A1} = \begin{cases} R_I - d \leq r \leq R_I, \theta_0(r) \leq \theta(r) \leq 2\pi - \theta_0(r) & \text{if } r_D \leq R_I, \\ R_I - d \leq r \leq r_D, \theta_0(r) \leq \theta(r) \leq 2\pi - \theta_0(r) & \text{if } R_I < r_D < R_I + d, \\ R_I - d \leq r \leq r_D, \begin{cases} \theta_0(r) \leq \theta(r) \leq 2\pi - \theta_0(r), \\ 0 \leq \theta(r) < 2\pi, \end{cases} \text{ for } r < R_I + d & \text{otherwise} \\ \mathcal{S}_c(d, r_E, R_I), & \text{if } R_I + d \leq r_D < r_I + R_p, \\ & \text{if } r_D \geq r_I + R_p. \end{cases}$$

▷ **Case 2:** $R_I \geq d$, $d + R_I \geq r_I + R_p$

$$\mathcal{S}_{A1} = \begin{cases} R_I - d \leq r \leq R_I, \theta_0(r) \leq \theta(r) \leq 2\pi - \theta_0(r) & \text{if } r_D \leq R_I, \\ R_I - d \leq r \leq r_D, \theta_0(r) \leq \theta(r) \leq 2\pi - \theta_0(r) & \text{if } R_I < r_D < r_I + R_p, \\ \mathcal{S}_c(d, r_E, R_I), & \text{if } r_D \geq r_I + R_p. \end{cases}$$


 Fig. 22. Illustration of \mathcal{S}_{A1} (Case 1)

▷ **Case 3:** $\frac{d}{2} < R_I < d$, $d + R_I < r_I + R_p$

$$\mathcal{S}_{A1} = \begin{cases} 0 \leq r \leq R_I, & \begin{cases} 0 \leq \theta(r) < 2\pi, & \text{for } r < d - R_I \\ \theta_0(r) \leq \theta(r) \leq 2\pi - \theta_0(r), & \text{otherwise} \end{cases}, & \text{if } r_D \leq R_I \\ 0 \leq r \leq r_D, & \begin{cases} 0 \leq \theta(r) < 2\pi, & \text{for } r < d - R_I \\ \theta_0(r) \leq \theta(r) \leq 2\pi - \theta_0(r), & \text{otherwise} \end{cases}, & \text{if } R_I < r_D < R_I + d \\ 0 \leq r \leq r_D, & \begin{cases} \theta_0(r) \leq \theta(r) \leq 2\pi - \theta_0(r), & \text{for } d - R_I < r < R_I + d \\ 0 \leq \theta(r) < 2\pi, & \text{otherwise} \end{cases}, & \text{if } R_I + d \leq r_D < r_I + R_p \\ \mathcal{S}_c(d, r_E, R_I), & & \text{if } r_D \geq r_I + R_p \end{cases}$$

▷ **Case 4:** $\frac{d}{2} < R_I < d$, $d + R_I \geq r_I + R_p$

$$\mathcal{S}_{A1} = \begin{cases} 0 \leq r \leq R_I, & \begin{cases} 0 \leq \theta(r) < 2\pi, & \text{for } r < d - R_I \\ \theta_0(r) \leq \theta(r) \leq 2\pi - \theta_0(r), & \text{otherwise} \end{cases}, & \text{if } r_D \leq R_I \\ 0 \leq r \leq r_D, & \begin{cases} 0 \leq \theta(r) < 2\pi, & \text{for } r < d - R_I \\ \theta_0(r) \leq \theta(r) \leq 2\pi - \theta_0(r), & \text{otherwise} \end{cases}, & \text{if } R_I < r_D < r_I + R_p \\ \mathcal{S}_c(d, r_E, R_I), & & \text{if } r_D \geq r_I + R_p \end{cases}$$

▷ **Case 5:** $R_I \leq \frac{d}{2}$, $d + R_I < r_I + R_p$

$$\mathcal{S}_{A1} = \begin{cases} 0 \leq r \leq R_I, 0 \leq \theta < 2\pi, & \text{if } r_D \leq R_I \\ 0 \leq r \leq r_D, 0 \leq \theta < 2\pi, & \text{if } R_I < r_D \leq d - R_I \\ 0 \leq r \leq r_D, \begin{cases} 0 \leq \theta(r) < 2\pi, & \text{for } r < d - R_I \\ \theta_0(r) \leq \theta(r) \leq 2\pi - \theta_0(r), & \text{otherwise} \end{cases}, & \text{if } d - R_I < r_D < R_I + d \\ 0 \leq r \leq r_D, \begin{cases} \theta_0(r) \leq \theta(r) \leq 2\pi - \theta_0(r), & \text{for } d - R_I < r < R_I + d \\ 0 \leq \theta(r) < 2\pi, & \text{otherwise} \end{cases}, & \text{if } R_I + d \leq r_D < r_I + R_p \\ \mathcal{S}_c(d, r_E, R_I), & \text{if } r_D \geq r_I + R_p \end{cases}$$

▷ **Case 6:** $R_I \leq \frac{d}{2}$, $d + R_I \geq r_I + R_p$

$$\mathcal{S}_{A1} = \begin{cases} 0 \leq r \leq R_I, 0 \leq \theta < 2\pi, & \text{if } r_D \leq R_I \\ 0 \leq r \leq r_D, 0 \leq \theta < 2\pi, & \text{if } R_I < r_D \leq d - R_I \\ 0 \leq r \leq r_D, \begin{cases} 0 \leq \theta(r) < 2\pi, & \text{for } r < d - R_I \\ \theta_0(r) \leq \theta(r) \leq 2\pi - \theta_0(r), & \text{otherwise} \end{cases}, & \text{if } d - R_I < r_D < r_I + R_p \\ \mathcal{S}_c(d, r_E, R_I), & \text{if } r_D \geq r_I + R_p \end{cases}$$

3) $\mathcal{S}_{A2} = \mathcal{S}_c(d, r_D, R_I) \cap \mathcal{S}_c(d, r_I + R_p, R_I)$:

▷ **Case 1:** $R_I \geq d$, $d + R_I < r_I + R_p$

$$\mathcal{S}_{A2} = \begin{cases} \phi & \text{if } r_D \leq R_I - d \\ R_I - d \leq r \leq r_D, \theta_0(r) \leq \theta(r) \leq 2\pi - \theta_0(r) & \text{if } R_I - d < r_D < R_I + d \\ R_I - d \leq r \leq r_D, \begin{cases} \theta_0(r) \leq \theta(r) \leq 2\pi - \theta_0(r), & \text{for } r < R_I + d \\ 0 \leq \theta(r) < 2\pi, & \text{otherwise} \end{cases}, & \text{if } R_I + d \leq r_D < r_I + R_p \\ \mathcal{S}_c(d, r_E, R_I), & \text{if } r_D \geq r_I + R_p \end{cases}$$

▷ **Case 2:** $R_I \geq d$, $d + R_I \geq r_I + R_p$

$$\mathcal{S}_{A2} = \begin{cases} \phi & \text{if } r_D \leq R_I - d \\ R_I - d \leq r \leq r_D, \theta_0(r) \leq \theta(r) \leq 2\pi - \theta_0(r) & \text{if } R_I - d < r_D < r_I + R_p \\ \mathcal{S}_{A1}, & \text{if } r_D \geq r_I + R_p \end{cases}$$

▷ **Case 3:** $R_I < d$, $d + R_I < r_I + R_p$

$$\mathcal{S}_{A2} = \begin{cases} 0 \leq r \leq r_D, 0 \leq \theta < 2\pi, & \text{if } r_D \leq d - R_I \\ 0 \leq r \leq r_D, \begin{cases} 0 \leq \theta(r) < 2\pi, & \text{for } r < d - R_I \\ \theta_0(r) \leq \theta(r) \leq 2\pi - \theta_0(r), & \text{otherwise} \end{cases}, & \text{if } d - R_I < r_D < R_I + d \\ 0 \leq r \leq r_D, \begin{cases} \theta_0(r) \leq \theta(r) \leq 2\pi - \theta_0(r), & \text{for } d - R_I < r < R_I + d \\ 0 \leq \theta(r) < 2\pi, & \text{otherwise} \end{cases}, & \text{if } R_I + d \leq r_D < r_I + R_p \\ \mathcal{S}_c(d, r_E, R_I), & \text{if } r_D \geq r_I + R_p \end{cases}$$

▷ **Case 4:** $R_I < d$, $d + R_I \geq r_I + R_p$

$$\mathcal{S}_{A2} = \begin{cases} 0 \leq r \leq r_D, 0 \leq \theta < 2\pi, & \text{if } r_D \leq d - R_I \\ 0 \leq r \leq r_D, \begin{cases} 0 \leq \theta(r) < 2\pi, & \text{for } r < d - R_I \\ \theta_0(r) \leq \theta(r) \leq 2\pi - \theta_0(r), & \text{otherwise} \end{cases} & \text{if } d - R_I < r_D < r_I + R_p \\ \mathcal{S}_c(d, r_E, R_I), & \text{if } r_D \geq r_I + R_p \end{cases}$$

C. Expression for $I(r_D, r_I, R_p)$

Recall that

$$I(r_D, r_I, R_p) = \int_0^{r_D} 2r \frac{\mathcal{S}_I(r, r_I, R_p)}{\pi R_p^2} dr$$

By using the expressions of $\mathcal{S}_I(r, r_I, R_p)$ in Appendix A and figuring out the integral in the above expression, we can obtain the closed-form expression as below.

□ **Case 1** ($r_I \leq R_p$):

- $r_D \leq R_p - r_I$

$$I(r_D, r_I, R_p) = \frac{r_I^2 r_D^2}{R_p^2}$$

- $r_D \geq R_p + r_I$

$$I(r_D, r_I, R_p) = r_I^2$$

- $R_p - r_I < r_D < R_p + r_I$

$$\begin{aligned} & I(r_D, r_I, R_p) \\ &= \frac{1}{2} r_I^2 + \frac{r_D^2}{\pi} \arccos\left(\frac{R_p^2 + r_D^2 - r_I^2}{2R_p r_D}\right) \\ &+ \frac{r_I^2 r_D^2}{\pi R_p^2} \arccos\left(\frac{r_I^2 + r_D^2 - R_p^2}{2r_I r_D}\right) - \frac{r_I^2}{\pi} \arcsin\left(\frac{r_I^2 + R_p^2 - r_D^2}{2r_I R_p}\right) - \frac{r_D^2 + r_I^2 + R_p^2}{4\pi R_p^2} \\ &\cdot \sqrt{(r_I + R_p + r_D)(r_I + R_p - r_D)(r_I - R_p + r_D)(R_p - r_I + r_D)} \end{aligned}$$

□ **Case 2** ($r_I > R_p$):

- $r_D \leq r_I - R_p$

$$I(r_D, r_I, R_p) = r_D^2$$

- $r_D \geq r_I + R_p$

$$I(r_D, r_I, R_p) = r_I^2$$

- $r_I - R_p < r_D < r_I + R_p$

The same as Case 1 ($R_p - r_I < r_D < R_p + r_I$)

REFERENCES

- [1] Q. Zhao and B. Sadler, "A Survey of Dynamic Spectrum Access: Signal Processing, Networking, and Regulatory Policy," *IEEE Signal Processing magazine*, vol. 24, pp. 79–89, May 2007.
- [2] J.F.C.Kingman, "Poisson Processes," Clarendon Press, Oxford, 1993.
- [3] Q. Zhao, "Spectrum Opportunity and Interference Constraint in Opportunistic Spectrum Access," *Proc. of ICASSP*, April, 2007.
- [4] Artemas Martin, "To find the Area Common to Two Intersecting Circles," *the Analyst*, vol. 1, No. 2, pp. 33-34, Feb. 1874.
- [5] Q. Zhao, W. Ren and A. Swami, "Spectrum Opportunity Detection: How Good is Listen-before-Talk?" in *Proc. of IEEE Asilomar Conference on Signals, Systems, and Computers*, November, 2007 (invited).